3-1-2013

Rearrangement of Cyclotriveratrylene (CTV) Diketone: 9,10-Diarylanthracenes with OLED Applications

Samuel R. Sarsah
Loyola University Chicago

Marlon R. Lutz Jr.
Loyola University Chicago

Matthias Zeller
Youngstown University

David S. Crumrine
Loyola University Chicago

Daniel Becker
Loyola University Chicago, dbecke3@luc.edu

Rearrangement of Cyclotriveratrylene (CTV) Diketone: 9,10-Diarylanthracenes with OLED Applications

Samuel R.S. Sarsah,[†] Marlon R. Lutz Jr.,[†] Matthias Zeller,[‡] David S. Crumrine,[†] and Daniel P. Becker[†]*

†Department of Chemistry, Loyola University Chicago, 1032 West Sheridan Road, Chicago, Illinois 60660,United States, and ‡Department of Chemistry, 1 University Plaza, Youngstown State University, Youngstown, Ohio 44555-3663, United States

Corresponding author E-mail: dbecke3@luc.edu

Abstract: Electroluminescent 9,10-diaryl anthracenes have been shown to be promising host and hole-transporting materials in organic electroluminescence due to their high thermal stability, electrochemical reversibility and wide band gap useful for organic light emitting diodes (OLEDs), especially blue OLEDs. Oxidation of cyclotriveratrylene (CTV) to the corresponding diketone and subsequent bromination resulted in an unexpected rearrangement to a highly functionalized 9-aryl-10-bromoanthracene derivative, which was employed in Suzuki couplings to synthesize a series of 9,10-diaryl compounds that are structural analogs of anthracene derivatives used in the preparation of OLEDs, but are more highly functionalized, including electron-donating methoxy groups in addition to substitution by a carboxylic acid moiety. The UV/fluorescence solution spectra show strong emissions at a 446 nm, 438 nm and 479 nm, respectively, for the anthracene 10-phenyl, 10-naphthyl and 10-pyrenyl adducts containing a benzoic acid functional group, whereas the analogs bearing the hydroxymethylene moiety from reduction of the benzoic acid to the corresponding alcohols gave much shorter emission wavelengths of 408 nm, 417 nm, and 476 nm, respectively, and had somewhat higher quantum yields, suggesting they are better candidates for OLED applications.

Introduction

The discovery and development of new materials for use in displaying electronic information has been essential in flat panel displays in today's ubiquitous portable devices and common every-day technologies including cell phones, flat-screen televisions, and ambient lighting.[1] The development of organic light-emitting diodes (OLEDs)[2] holds great promise for the production of highly efficient light sources, with the advantage that they can be more economical to use and they can exhibit electroluminescence at relatively low voltages, making them exceptionally useful for application in electronic devices.[3,4] It is desirable that compounds used in OLEDs have good morphological properties including a good film forming ability, an amorphous or non-crystalline solid state, good thermal stability characterized by high decomposition temperatures, and a narrow HOMO-LUMO energy band gap in order to function in OLEDs. Red and green color electroluminescence are relatively easy to obtain from OLEDs, but blue color emitters are rare and tend to degrade rapidly due to the larger energy band gap required for blue color emission. This has triggered research into finding more stable organic compounds that can be used for making efficient OLED devices, especially for blue OLEDs.

The wide energy band gap of electroluminescent anthracene compounds makes them potentially useful for organic light emitting diodes, especially blue OLEDs,[5] and 9,10-diarylanthacenes (Figure 1) are important blue host emitters in the preparation of OLEDs, including 9,10-diphenylanthracene (DPA)[6] and 9,10-di-(2-naphthyl)anthracene (ADN).[7] Known 9,10-diarylanthracene host emitters that contain a 2-tert-butyl group[8] include 2-*tert*-butyl-9,10-bis-(â-naphthyl)-anthracene (DBADN),[9] 2-tert-butyl-9,10-di(9-phenanthryl) anthracene (TBDHA),[10] and 2-tert-butyl-9,10-di(1-pyryl)anthracene (TBDPA).[10] More highly functionalized 9,10-diaryl anthracenes have also been described in recent disclosures.[11-13] Three deep-blue-emitting anthracene derivatives, 2-tert-butyl-9,10-bis(9,9-dimethylfluorenyl) anthracene (TBMFA), 2-tert-butyl-9,10-bis[4-(2-naphthyl)phenyl] anthracene (TBDNPA), and 2-tert-butyl-9,10-bis[4-(9,9-dimethylfluorenyl)phenyl] anthracene (TBMFPA), with naphthalene or 9,9-dimethylfluorene side units were recently reported,[13] where amorphous thin film forming

derivatives are enabled by effectively introducing alkyl substituents in the compounds to prevent the molecules from easily packing to form crystals in thin films.[8, 14] Bulky substituents on the anthracene moieties can improve both thermal and film forming properties.[10]

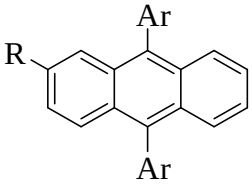

DPA	R = H	Ar = phenyl
ADN	R = H	Ar = 2-naphthyl
TBADN	R = t-butyl	Ar = 2-naphthyl
TBDHA	R = t-butyl	Ar = 9-phenanthryl
TBDPA	R = t-butyl	Ar = 1-pyrenyl

Figure 1. 9,10-Diarylanthracene derivatives used as blue host emitters for OLEDs

Results and Discussion

Part of our research program is focused on the construction of apex-modified derivatives[15-17] of the trimeric crown-shaped (bowl-shaped) [1.1.1]orthocyclophane cyclotriveratrylene **1** (CTV, Figure 2)[18] with applications in host-guest chemistry.[19] Trans-annular rearrangements are known to occur when attempting to oxidize CTV-5,10-dione **1c** to the corresponding triketone which leads to rearrangement to the spiro derivative **2**,[20, 21] and we have observed a trans-annular electrophilic aromatic addition or substitution cascade following a Beckmann rearrangement reaction on a related system.[22] We examined the bromination of CTV 5,10-dione, indeed trying to avoid the formation of spiro derivative **2**, which resulted instead in a rearrangement to the highly functionalized 9-aryl-10-bromo anthracene derivative **3a**. Specifically, treating CTV diketone **1c** with *N*-bromosuccinimide in the presence of benzoyl peroxide in 1,2-dichloroethane at 70°C for 5h afforded a 77% yield of bromoanthracene benzoic acid **3a**. When the reaction was performed in chloroform, the ethyl ester **3b** was also isolated with a significant NMR upfield shift for the methyl hydrogen atoms due to anisotropy [δ = 0.31 (3H, t, J = 7.14 Hz)], arising from acid-catalyzed esterification of the acid with ethanol present in commercial chloroform as a stabilizer. The exact identities of both **3a** and **3b** have been confirmed by single-crystal X-ray analysis (Figures 3, S1 and S2, Table S1).

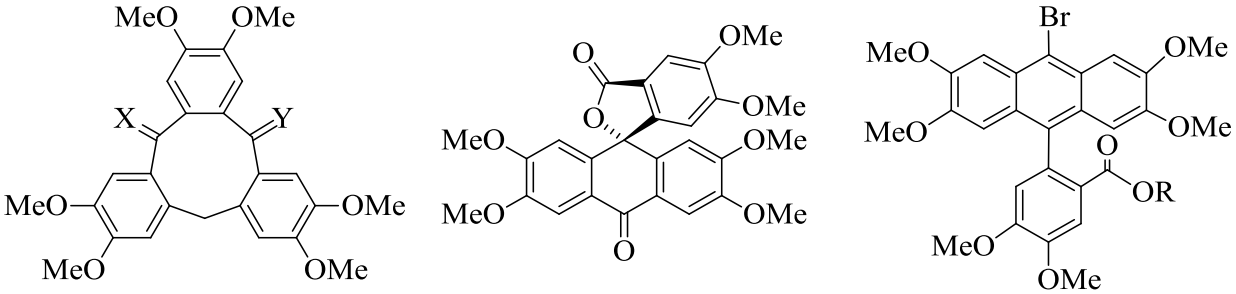

1a CTV X,Y = H,H

1b CTV ketone X = O; Y = H,H

1c CTV diketone X,Y = O

2

3a R = H

3b R = ethyl

Figure 2. CTV and related structures

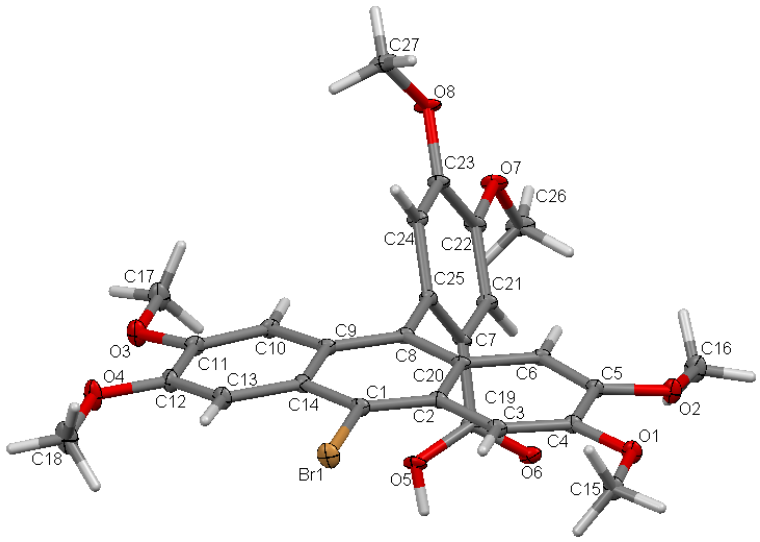

Figure 3. Single crystal X-ray structure of bromoanthracene benzoic acid **3a**, 50% thermal probability ellipsoids. A solvate dichloromethane molecule is omitted for clarity. For details of the structure analyses of **3a** and **3b**, see the supporting information (Figures S1 and S2, Table S1).

Given the interest in 9,10-diaryl anthracenes as hole transporting materials in organic electroluminescence along with their great importance in the preparation of OLEDs, and realizing that the 9-bromo substituent of anthracene **3a** lends itself directly to the installation of a second aryl substituent on the anthracene via palladium catalyzed coupling reactions, we were excited to explore the effect of different substituents on the optical properties of this type of compound. Thus, we set out to determine the utility of 10-bromoanthracene **3a** toward the

preparation of 9,10-diaryl anthracenes with potential applications in the preparation of OLEDs. To this end, Suzuki couplings were used to link bromoanthracene **3a** with phenyl, 2-naphthyl, and 1-pyrenyl boronic acids to form 9,10-substituted anthracene derivatives **4a**, **4b** and **4c**, respectively (Scheme 1).

Suzuki coupling of **3a** with phenylboronic acid with a catalytic amount of tetrakistriphenylphosphine palladium and sodium carbonate in ethanol/toluene at 115°C for 24 h gave only a trace of coupled material. The stronger base sodium hydroxide in ethanol/n-butanol at 90-100°C for 24 h, however, gave **4a** (R = Ph) in 29% yield, whereas utilization of Pd(0)-catalyzed coupling with the milder base potassium fluoride in the presence of silver(I) oxide[23-25] in 2-methoxyethanol with THF to aid solubility gave **4a** in an excellent yield (96%). Similarly, Suzuki coupling of 2-naphthylboronic acid utilizing sodium hydroxide as the base in ethanol gave **4b** in 21% yield along with a significant amount of hydrolytic deboronation[26] as well as the typical dehalogenation, but the KF/Ag_2O procedure gave **4b** in 88% isolated yield. Coupling with pyrene-1-boronic acid to afford **4c** was more sluggish, suffering from more deboronation, and giving only a trace of coupled material with NaOH/EtOH, but afforded an isolated yield of 48% with KF/Ag_2O. An upfield shift in the ^{1}H NMR resonances of the methoxy groups proximal to the added phenyl, naphthyl and pyrenyl groups is observed upon replacement of the bromine in the Suzuki couplings. For adduct **4c** with the larger pyrenyl substituent, hindered rotation of the pyrene versus the dimethoxy benzoic acid moiety leads to formation of two atropisomers[27] which were separated by preparative plate chromatography. The two compounds have nearly identical UV and fluorescence spectra, but the individual ^{1}H NMR spectra show that the methoxy groups proximal to the pyrene differ by 0.018 ppm. These two peaks in the unseparated mixture of atropisomers integrate in a ratio of 1:1 demonstrating the existence of equal amounts of each atropisomer at room temperature. Variable temperature NMR in d_6-DMSO showed no interconversion up to 100°C, and semi-empirical AM1 calculations of the equilibrium geometries show that the two atropisomers differ by only 0.036 kcal/mol.

Scheme 1. Suzuki couplings to prepare 9,10-diaryl anthracenes **4a-4c** and reduction to benzyl alcohols **5a-c**

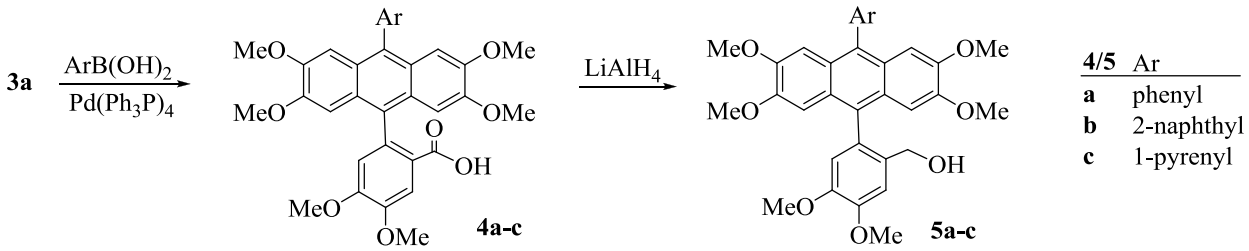

UV/vis and fluorescence spectra were obtained for all three acids **4a-c** and the three corresponding alcohols **5a-c** in both dichloromethane solution and in the solid state. In dichloromethane solution, the three benzoic acids **4a-c** each show nearly identical UV absorption maxima at 278 (ε ~8 x 10^4) and 378 (ε~1 x 10^4) nm (Figure 4) corresponding to two π–π* excitations. The UV spectra of **4a-b** are very similar to the UV spectrum of anthracene due to minimal conjugation of the twisted aryl substituents at the 9- and 10- substituents that have been reported[28,29] to be rotated by about 66° with respect to the anthracene core in the ground state of 9,10-diphenylanthracene. The UV spectra of the two pyrenyl derivatives **4c** show absorptions for both the anthracene moiety at 276 nm and 372 nm, and for the pyrene moiety at 245, 276, 327, 341, and 368 nm. The onset of absorption for the phenyl derivative **4a** and naphthyl derivative **4b** are both red shifted by modest conjugation with the anthracene. The pyrenyl derivatives **4c** were the most red shifted and also had the smallest energy band gap. The solid state UV/Vis spectra of the phenyl and naphthyl substituted acids **4a** and **4b**, respectively, showed a slight red shift in the long wave absorption maxima when compared to their solution spectra. The long wavelength maxima of the pyrenyl substituted acid **4c** and the corresponding alcohols all show blue shifts.

With 375 nm excitation, all of these compounds show unstructured blue fluorescence at 10^{-5} M in dichloromethane solution. The lack of vibronic structure in the fluorescence suggests some degree of electronic interaction between the two π systems.[30] Phenyl derivative **4a,** (Fig. 4), provided unstructured fluorescence emission with a 446 nm maximum, while naphthyl derivative **4b** showed unstructured fluorescence with a 438 nm maximum. This lower energy emission in **4a** can be explained if the barrier to excited state rotational relaxation about the anthracene-naphthyl bond in **4b** is greater than the excited state rotational barrier of the anthracene-phenyl bond in **4a**. This is not surprising since we isolated atropisomers of the pyrenyl substituted **4c**,

which means it has a very high ground state barrier to rotation. The longer wavelength fluorescence maximum in the phenyl derivative **4a** then reflects a lower energy flatter excited state conformation with respect to **4b**.[31]

In pyrenyl system **4c**, the unstructured fluorescence maximum in dichloromethane is 479 nm. This is quite red shifted compared to the fluorescence of 1-phenylpyrene[30] and even more red shifted than the fluorescence of 1-(9-anthracenyl)pyrene in acetonitrile which was attributed to charge transfer interactions.[32] This suggests that the fluorescence of **4c** has a large component of charge transfer interactions. We know from the **4c** atropisomers that we isolated that the ground state barrier to rotation is large, so **4c** isomers have the least ground state π overlap between the aromatic systems of these derivatives. The solid state fluorescence maxima of the acids were all blue shifted compared to their solution state fluorescence spectra, whereas the solid state fluorescence maxima of the phenyl and naphthyl substituted benzyl alcohols were red shifted, but the fluorescence maximum of the pyrenyl substituted benzyl alcohol was blue shifted, again in comparison to the corresponding solution fluorescence maxima.

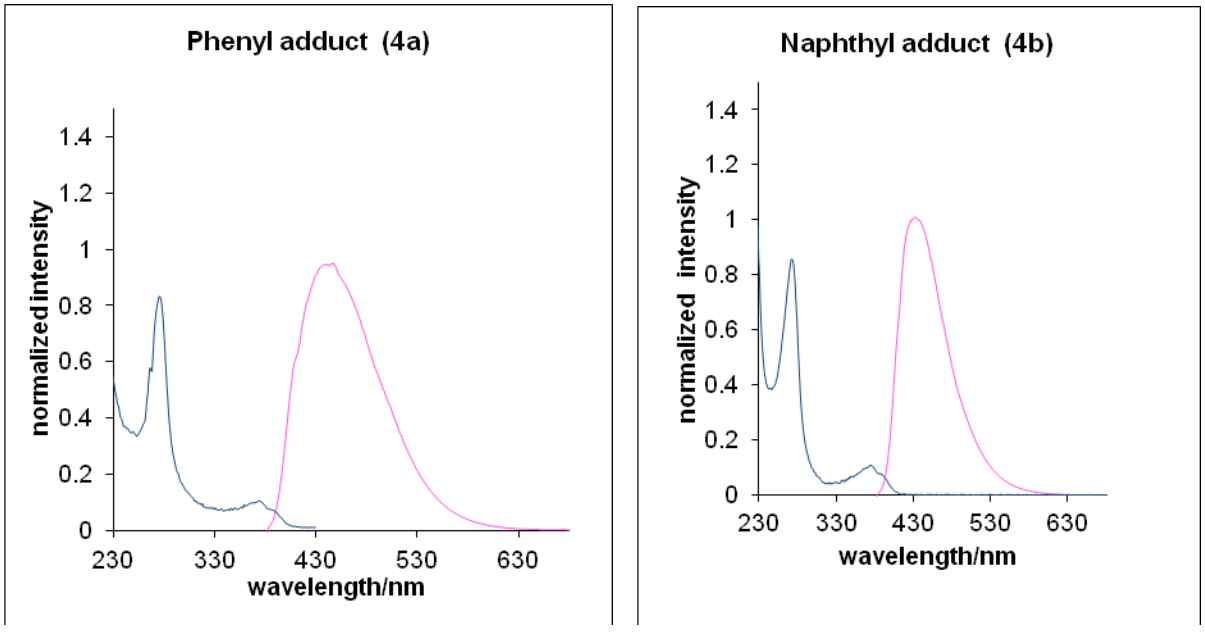

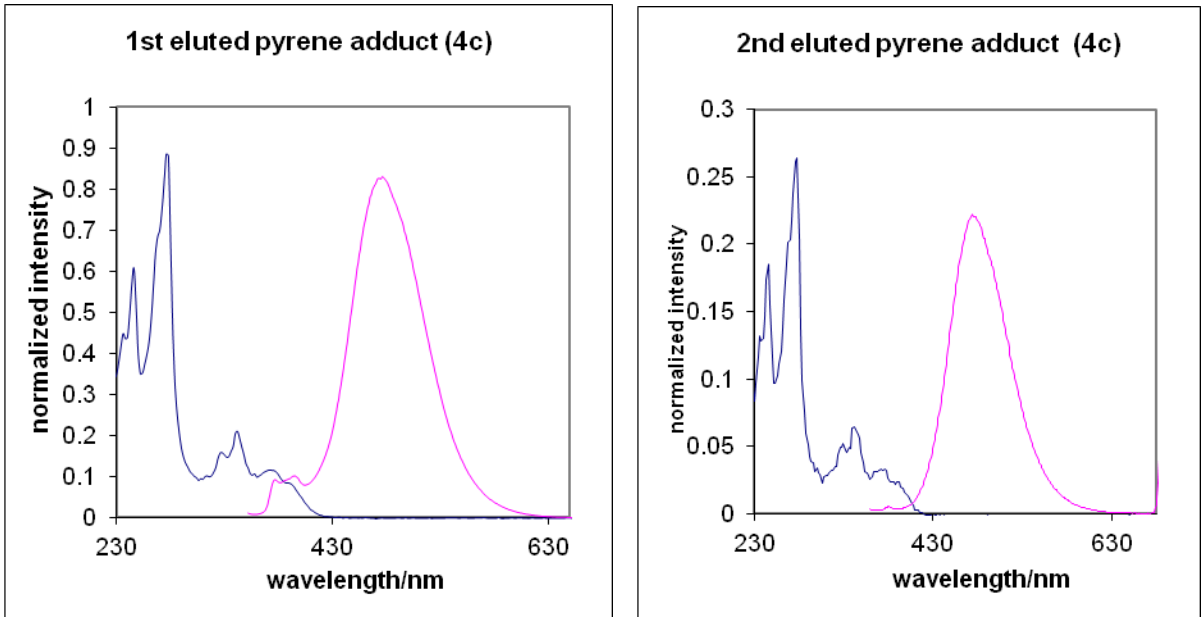

Figure 4. UV/fluorescence solution spectra of compounds **4a-c**. The UV trace shown in magenta; the fluorescence trace is shown in dark blue. All spectra were recorded at a concentration of 8.6 x 10^{-6} M in dichloromethane at room temperature. Spectra were recorded in dichloromethane at the following concentrations and excitation wavelengths: 10-phenyl adduct **4a** at 8.6 x 10^{-6} M, excitation wavelength 374 nm; 10-naphthyl adduct **4b** at 4.3 x 10^{-6} M, excitation wavelength 374 nm; 10-pyrenyl adduct **4c** (1:1 mixture of atropisomers) at 4.3 x 10^{-6} M, excitation wavelength 372 nm; Anthracene at 7.166 x 10^{-7} M, excitation wavelength 377 nm.

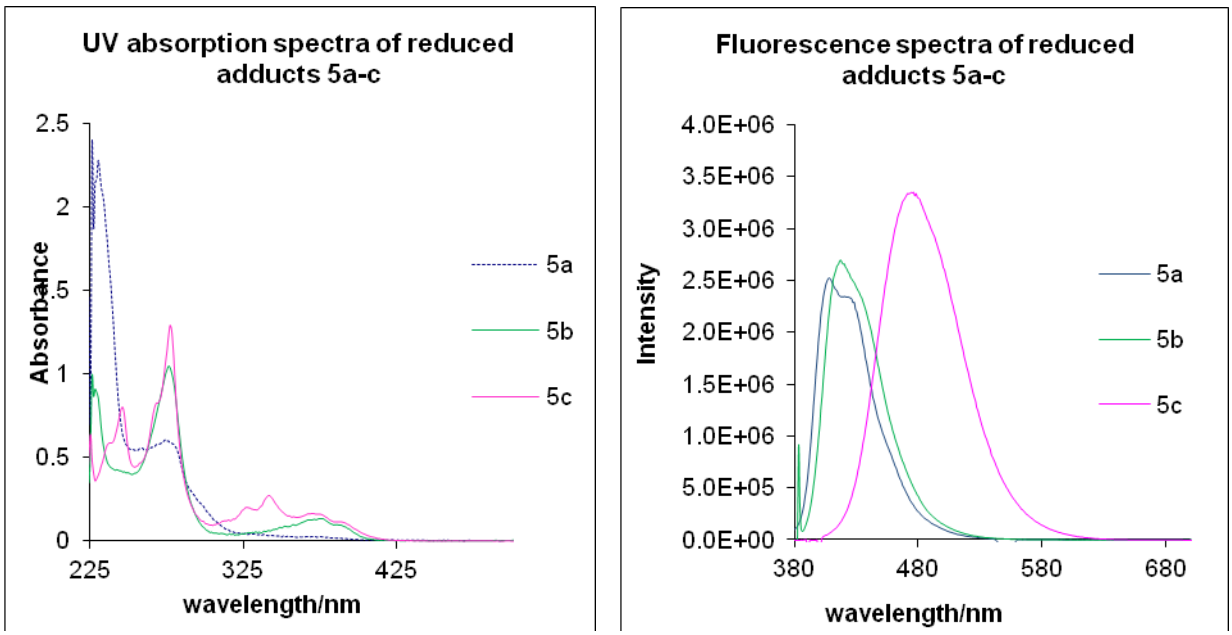

Figure 5. UV and fluorescence spectra of reduced adducts **5a-c**. Fluorescence spectra were recorded with excitation wavelengths of 274 nm, 377 nm and 395 nm, respectively, corresponding to the emission λ_{max} for **5a-c** at a concentration of 9.31 x 10^{-7} M, 2.38 x 10^{-7} M, and 8.6 x 10^{-7} M, respectively for **5a-c**.

We were concerned whether the presence of the electron-withdrawing benzoic acid moiety would reduce the quantum yields of solution fluorescence, so the benzoic acid group was converted to the corresponding alcohol by reduction with lithium aluminum hydride in tetrahydrofuran (Scheme 1).

Fluorescence quantum yields (Q_f) were measured using 365 nm excitation with absorbance in dichloromethane of about 0.0265 for all compounds. The fluorescence of anthracene (0.27 in ethanol) was the standard.[33-38] The alcohols **5a** and **5b** did exhibit a marked increase in solution state fluorescence quantum yields, although the pyrenyl alcohol **5c** was comparable to the parent carboxylic acid **4c**. The alcohols also exhibit lower emission wavelengths (are blue shifted) compared to the corresponding benzoic acid derivatives. The UV spectra show increased molar absorptivity at 274 nm, and this is reversed for the benzoic acids **4a-c** due to the presence of the carbonyl group in **4a-c** which can absorb a significant portion of the incident excitation energy through an n-π^* transition[39] and decreases the effective fluorescence emission and the quantum yields of compounds **4a-c**. The hydroxymethyl group is electron donating, resulting in increased wavelengths for the π-π^* transitions, and thereby increasing solution fluorescence quantum yields for **5a-c**. Absorption and fluorescence spectra of anthracene itself are mostly mirror symmetric. In contrast, the prepared derivatives (**4a-c**, **5a-c**) show a single emission peak. This is due to the rigid structure of anthracene compared to the derivatives described herein where large attached substituents result in increased vibrational degrees of freedom and increased vibronic coupling of the electronic energy levels in all the derivatives.[40]

The blue shifts for the solid state fluorescence maxima of acids **4a**, **4b**, and **4c**, in comparison to their solution state fluorescence maxima, suggest that, in these solid state excited states, there is less overlap between the aryl rings and the anthracene core. This could be understood if, in these solid state excited states, the barriers to rotation of the aryl rings toward coplanarity with the anthracene core are higher than the corresponding barriers for the solution state excited states.

The pyrenyl benzyl alcohol **5c** also shows a blue shift for the solid state fluorescence maxima. In contrast, the other two benzyl alcohols **5a** and **5b** show red shifts in their solid state fluorescence maxima.

The differences in the relative efficiencies of fluorescence in solution versus in the solid state are dramatic. In solution, the phenyl and naphthyl substituted benzyl alcohols have much higher quantum yields than the corresponding acids. In solution, both pyrenyl substituted molecules showed similar maxima that show considerable charge transfer character in the excited state. Their solution state fluorescence quantum yields were similar to each other, about three times the quantum yields for the phenyl and naphthyl acids and about one half of the value for the phenyl and naphthyl benzyl alcohols. We recorded the solid state fluorescence spectra of each compound and in Table 1 report the solid state fluorescence output as the product of the absorbance value at the wavelength of excitation (370 nm) and the integrated fluorescence intensity for each compound. It is clear that the phenyl substituted acid **4a** has the most intense fluorescence. The solid state fluorescence spectra were normalized by division of the product of absorbance time integrated fluorescence intensity for all of the other compounds by the product of absorbance time integrated fluorescence intensity for **4a**. Those ratios are shown on Table 1. The solid state fluorescence intensities of **4a** and **4b** are considerably larger than those for the other compounds.

Solid state fluorescence spectra are strongly influenced by intermolecular steric forces[41] and crystal structure which determine distance and orientation between neighboring molecules.[42-44] Changing substituents on molecules can change crystalline forms[45] and fluorescence efficiencies.[46] Thus, the differences in solid state fluorescence could be attributed to a greater angle between the core anthracene and the phenyl and naphthyl rings in the acids **4a** and **4b** which would then increase the distance between successive planes of solid molecules and increase the fluorescence efficiencies with respect to the solution efficiencies. On the other hand, the solid state UV spectra show slight red shifts for **4a** and **4b,** so we contine to look for the best explanation.

Table 1. Optical properties and melting points of 9,10-diarylanthracenes **4a-c** and **5a-c**

Cmpd	UV-Vis Soln λ_{max} (ε) (nm, 10^3 M^{-1} cm^{-1})	UV-Vis Thin film λ_{max} (nm)	Fluor max Soln (λ_{max} /nm)	Fluor max Thin film (λ_{max} /nm)	Rel fluor Soln (quantum yield,Q_f)	Rel fluor ratios Thin films	Abs energy band gap (nm, eV)	Solution Conc (10^{-7} M)	Mp (ºC)
4a	276 (96.8) 374 (12.3)	377	446	411	0.063	1.0	412 2.91	9.10	228-232
4b	273 (99.6) 375 (12.4)	378	438	428	0.058	0.37	418 2.87	3.98	234-240
4c	276 (83.8) 339 (18.7) 366 (10.2) 372 (10.8)	346	479	464	0.197	0.037	426 2.82	2.23	120-125 (Tg)
5a	274 (70.3) 359 (10.6)	377	408	428	0.325	0.040	401 2.99	9.31	197-203
5b	276 (122.0) 377 (15.3)	361	417	437	0.39	0.032	415 2.89	2.39	202-205
5c	277 (150.6) 322 (17.6) 338 (26.6) 370 (18.8) 381 (14.6)	346	476	447	0.17	0.029	420 2.86	1.26	115-120 (Tg)
anthr-cene	ND	ND	ND	ND	0.27 (EtOH)[36]	ND	ND	3.26	ND

ND = not determined

The band gap values were calculated from the wavelength at the onset of absorbance.

$$\nu = c/\lambda \text{.....(3)} \qquad h\nu = E_{HOMO}\text{-}E_{LUMO} \text{..... (4)}$$

where c is light velocity in vacuum, λ is the wavelength of the absorption onset, and h is Plank's constant.

In summary, we report the rearrangement of a CTV derivative to a highly functionalized 9-aryl-10-bromoanthracene derivative. From that bromoanthracene derivative, we have prepared a series of 9,10-diaryl derivatives utilizing Suzuki couplings. These Suzuki products were evaluated as the parent benzoic acids as well as their corresponding reduced alcohol derivatives by solution and solid state UV and fluorescence spectroscopy. We have measured the relative fluorescence quantum yields (Q_f) in addition to the absorption energy band gaps for each of the 9,10-diaryl anthracene derivatives. Several of these compounds with higher quantum yields, especially **5a** and **5b** (Q_f = 32.5% and 39%), show promise as hole transporting materials in organic electroluminescence for the construction of organic light emitting diodes (OLEDs), especially blue OLEDs.

Experimental Section

All solvents and reagents were used without further purification unless otherwise noted. Solvents used in the synthesis of the final compound were distilled from calcium hydride. Reactions were performed under an atmosphere of nitrogen. Silica gel 60 (230-400 mesh) was used for flash chromatography. Aluminum-backed silica gel plates (0.25 mm) were used for TLC. ^{1}H NMR spectra were obtained with either a 300 MHz, a 400 MHz, or a 500 MHz spectrometer with tetramethylsilane (TMS) as an internal standard. Noise-decoupled ^{13}C NMR spectra were recorded at 75 MHz or 125 MHz. IR spectra were recorded on an FT-IR using NaCl crystal polished optical discs, (25mm x 4mm). HRMS spectra were measured on a TOF instrument. UV-Vis spectra were obtained using an UV-Vis Spectrometer. Single crystal X-ray structures were collected on a CCD area detector X-ray diffractometer at 100 K. Solution UV absorbance spectra were measured with a UV-Visible spectrophotometer while the fluorescence was measured with a spectrofluorometer. Semi-empirical AM1 calculations were performed using Spartan 2003. For the solid state UV-fluorescence spectra, a solution of sample (1.0 mM) in dichloromethane was spin coated on thin glass slides in an evacuated chamber pre-flushed with nitrogen. UV spectra were recorded on a single beam array detector spectrophotomer. Fluorescence was recorded in a right angle mode with excitation at λ = 370 nm.

Relative fluorescence Quantum yields

Quantum yields (Q_f) were measured at an excitation wavelength of 365nm with an absorbance of about 0.0265 for all compounds in dichloromethane and were compared to anthracene in ethanol (Q_f = 0.27). $Q_f = (A_s/A_x)(I_x/I_s)(n_x/n_s)^2(0.27)$. The symbols A, I and n refer to the absorbance, integrated fluorescence intensity (area under the curve), and refractive indices of solvents dichloromethane (n_x=1.42) for compounds x and ethanol (n_s=1.38) for the anthracene standard solution respectively. The areas under the curve were measured using the ORIGINpro computer software.

(2,3,7,8,12,13)-Hexamethoxy-5H-tribenzo[a,d,g]cyclononene-5,10(15H)-dione (CTV-Diketone, 1c). To a 500-mL reactor charged with cyclotriveratrylene (CTV, **1a**; 4.28 g, 9.50 mmol) was added a finely ground uniform mixture of potassium permanganate (60 g, 380 mmol) and activated manganese dioxide (66.0 g, 760 mmol), and 120 mL of pyridine. The reaction mixture was stirred vigorously under reflux for 18 h. The reaction mixture was then vacuum filtered hot (90°C) through a bed of Celite. The reactor and Celite bed were rinsed with ethyl acetate followed by dichloromethane (100 mL ea). The organic solvent was removed *via* reduced pressure (50°C, 10 mm Hg). The crude material was further dried *in vacuo* at 100°C for 1 h to give a pale yellow solid (3.62 g). Chromatography on silica gel (40:1 loading ratio) eluting with methylene chloride followed by a step gradient of ethyl acetate/methylene chloride (5/95 to 50/50) afforded CTV-monoketone **1b**[20,47] (1.40 g, 32%) followed by CTV-diketone **1c**[48] (1.88 g, 41%): mp 138-144°C ^{1}H NMR of **1c** δ 7.20 (2H, s), 6.98 (2H, s), 6.52 (2H, s), 3.92 (12H, s), 3.88 (2H, bs), 3.86 (6H, s). ^{13}C NMR δ 196.2, 151.7, 150.2, 147.5, 135.2, 133.6, 131.1, 111.7, 111.3, 109.5, 109.4, 55.8, 55.7, 55.7, 55.6, 55.6.

2-(10-Bromo-2,3,6,7-tetramethoxyanthracen-9-yl)-4,5-dimethoxybenzoic acid (3a). CTV-diketone **1c** (256 mg, 0.535 mmol) was added to *N*-bromosuccinimide (95.2 mg, 0.535 mmol) and benzoyl peroxide (1.3 mg, 0.0046 mmol) dissolved in 1,2-dichloroethane (3 mL) and heated to 70°C for 2 h and then cooled to room temperature, diluted with 20 mL de-ionized water, and acidified to pH 2-3 using conc hydrochloric acid. The resulting mixture was extracted with dichloromethane (3 × 40 mL) and the combined organic layers were washed with brine (3 × 40 mL) and dried over $MgSO_4$. Concentration under reduce pressure afforded a residue which was purified by silica gel column chromatography eluting with ethyl acetate/dichloromethane to afford bromoanthracene **3a** (231 mg, 77%): mp 224-226°C. ^{1}H NMR δ 7.73 (1H, s), 7.71 (2H, s), 6.73 (1H, s), 6.53 (2H, s), 4.10 (6H, s), 4.03 (3H, s), 3.83 (3H, s), 3.69 (6H, s). ^{13}C NMR δ 169.9, 153.0, 150.7, 149.6, 148.4, 135.2, 132.9, 126.52, 126.48, 122.5, 118.2, 114.9, 114.0, 105.6, 103.9, 56.6, 56.4, 56.2, 56.0. The benzoic acid proton was not observed due to exchange with water. The structure was ultimately confirmed by X-ray crystallography (CH_2Cl_2/heptane) as seen in Fig 3 (and Fig S1, Table S1).

2-(10-Bromo-2,3,6,7-tetramethoxyanthracen-9-yl)-4,5-dimethoxybenzoic acid (3a) and 2-ethyl (10-bromo-2,3,6,7-tetramethoxyanthracen-9-yl)-4,5-dimethoxybenzoate (3b). A vial was charged with CTV diketone **1c** (95.6 mg, 0.20 mmol), *N*-bromosuccinimide (35.6 mg, 0.20 mmol), benzoyl peroxide (0.5 mg, 0.002 mmol), and chloroform (1.1 mL). The reaction was stirred at 70°C for 5.5 h, during which time the reaction solution had turned from an orange to a dark brown. The mixture was then cooled to room temperature and diluted with deionized water (5 mL) and methylene chloride (5 mL), and the pH was adjusted to pH 10-11 with 2M aqueous sodium hydroxide solution. The aqueous layer was extracted with methylene chloride (2 × 5 mL). The combined organic layers were successively washed with brine and dried over sodium sulfate. Concentration under reduced pressure (10 mm Hg) gave 93 mg of crude material. Purification *via* column chromatography on silica gel (50:1 loading ratio) eluting with methylene chloride followed by an ethyl acetate/methylene chloride gradient (0/100 to 20/80, then 30/70 containing 3% AcOH) afforded the ethyl ester **3b** (21.3 mg, 18.4%): mp 261-263°C; ^{1}H NMR δ 7.77 (1H, s), 7.72 (2H, s), 6.81 (1H, s), 6.62 (2H, s), 4.11 (6H, s), 4.09 (3H, s), 3.87 (3H, s), 3.74 (6H, s), 3.66 (2H, q, J = 7.14 Hz), 0.31 (3H, t, J = 7.14 Hz). ^{13}C NMR δ 166.8, 152.2, 150.6, 149.4, 148.4, 133.9, 133.6, 126.5, 126.4, 124.4, 117.6, 114.7, 114.6, 113.5, 113.4, 105.5, 105.4, 104.1, 104.0, 60.6, 56.5, 56.4, 56.3, 56.1, 56.0, 55.9. The identity of **3b** was ultimately confirmed by X-ray crystallography (Fig S2, Table S1). Continued elution yielded the free acid **3a** (46.6 mg, 58.3%) which was identical to the material prepared in 1,2-dichloroethane above. Continued elution afforded a very small amount of the spirolactone derivative **2** (2.3 mg, 2.4%) which was identical to material reported in the literature.[20, 21]

4,5-Dimethoxy-2-(2,3,6,7-tetramethoxy-10-phenylanthracen-9-yl) benzoic acid (4a). Bromo-anthracene **3a** (154 mg, 0.28 mmol), $Pd(PPh_3)_4$, (971 mg, 30 mol%), phenyl boronic-acid (102.4 mg, 0.84 mmol) potassium fluoride (97 mg,1.68 mmol) and silver (I) oxide (71.4 mg, 0.308 mmol) was added to 2-methoxyethanol (0.5 mL) and THF (0.5 mL). The mixture was degassed by flushing under nitrogen and heated in a sealed tube at 90-100°C for 24 h. The reaction mixture was allowed to cool to room temperature and diluted with 20 mL cold de-ionized water. It was then acidified with conc HCl to pH 2-3 and extracted four times with 20 mL of dichloromethane. The combined organic layers were washed twice with water (40 mL), dried

over anhydrous Na_2SO_4, concentrated under reduced pressure and the raw material was purified by silica gel chromatography using methylene chloride/ethyl ether and ethyl ether /ethyl acetate : 100/0 to 10 /100 with 10 % increments for each ratio to afford 10-phenyl anthracene **4a** as a light orange solid (72 mg, 96%): ^{1}H NMR δ 7.81 (1H, s), 7.75-7.40 (6H, m), 6.83 (1H, s), 6.81 (2H, s), 6.61 (2H, s), 4.07 (3H, s), 3.86 (3H, s), 3.71 (6H, s). ^{13}C NMR δ 168.5, 152.8, 149.2, 148.8, 148.1, 139.6, 139.1, 135.3, 133.4, 131.3, 131.1, 130.9, 128.68, 128.66, 127.5, 125.80, 125.76, 125.70, 122.4, 114.9, 113.8, 104.1, 103.2, 56.3, 56.1, 55.6, 55.5. ESI HRMS m/z calcd for M-1 $C_{33}H_{29}O_8$ 553.1862, found 553.1833. FTIR (neat): ν 3527 (br), 2999, 2936, 2831, 1491, 1238 cm^{-1}; Td = 381.2°C

4,5-Dimethoxy-2-(2,3,6,7-tetramethoxy-10-(naphthalen-2-yl)anthracen-9-yl)benzoic acid (4b). Bromo-anthracene **3a** (156 mg, 0.280 mmol), $Pd(PPh_3)_4$ (97.1 mg, 0.084 mmol), naphthyl-2- boronic-acid (145 mg, 1.40 mmol) potassium fluoride (60 mg, 1.68 mmol) and silver (I) oxide (71.4 mg, 0.308 mmol) were added to a mixture of 2-methoxyethanol (4.5 mL) and THF (6.5 mL). The mixture was degassed by flushing under nitrogen and heated in a sealed tube at 90-100°C for 48 h. The reaction mixture was allowed to cool to room temperature and diluted with cold de-ionized water (20 mL). It was then acidified with conc HCl to pH 2-3 and then extracted with dichloromethane (4 × 20 mL). The combined organic layers were washed with water (2 × 40 mL) and dried with Na_2SO_4. The solution was then concentrated under reduced pressure and purified by silica gel chromatography using methylene chloride/ethyl ether followed by ethyl ether /ethyl acetate (100% to 10 % with 10 % increments for each interval) to afford naphthyl derivative **4b** as a light tan solid (111 mg, 88%): ^{1}H NMR δ 8.1–7.9 (4H, m), 7.80 (1H, s), 7.70-7.55 (3H, m), 6.80 (3H, s), 6.60 (2H, s), 4.06 (3H, s), 3.9 (3H, s), 3.7 (6H, s), 3.6 (6H,s). ^{13}C NMR δ 170.2, 153.0, 149.3, 149.2, 148.3, 137.6, 137.4, 135.8, 135.8, 133.9, 133.1, 133.1, 133.0, 133.0, 132.2, 130.4, 130.2, 129.8, 129.6, 128.5, 128.4, 128.3, 128.2, 128.1, 126.6, 126.5, 126.4, 125.9, 122.8, 115.2, 114.0, 104.3, 103.6, 56.6, 56.4, 55.9, 55.8. MS-TOF calcd for $C_{37}H_{32}O_8$ 604.21, found m/z 603.3 (M-1); HRMS ESI calcd for MH^+ $C_{37}H_{33}O_8$ 605.2175, found 605.2163. FTIR (neat): ν 3526 (br) 2935, 2831, 1491, 1237 cm^{-1}. Tg = 143.5°C.

4,5-dimethoxy-2-(2,3,6,7-tetramethoxy-10-(pyren-1-yl)anthracen-9-yl)benzoic acid (4c). Bromo-anthracene **3a** (100 mg, 0.179 mmol), Pd $(PPh_3)_4$, (75.2 mg, 0.065 mmol), pyrene-1-boronic-acid (199 mg, 0.809 mmol), potassium fluoride (93.9 mg, 1.62 mmol) and silver (I) oxide (50.3 mg, 0.217 mmol) were added to 2-methoxyethanol (25 mL). The mixture was degassed by flushing with nitrogen and heated in a sealed tube at 130°C for 48 h. The reaction was allowed to cool to room temperature and diluted with 20 mL cold de-ionized water, and then acidified with concentrated HCl to pH 2-3 and then extracted four times with 20 mL of dichloromethane. The combined organic layers were washed twice with water (40 mL) and dried over anhydrous Na_2SO_4. Concentration under reduced pressure and purification of the resulting residue by silica gel chromatography eluting with methylene chloride/ethyl ether followed by ethyl ether /ethyl acetate (100% to 10 % with 10 % increments for each interval) afforded pyrenyl derivative **4c** (95.5mg, 79%) as a light cream-colored solid: ^{1}H NMR (mixture of atropisomers; doubled peaks noted) δ 8.42–8.40 and 8.41–8.38 (1H, 2d, J=7.8Hz), 8.28-8.01 (8H, m), 7.90 (1H, s), 7.86-7.83 and 7.85-7.82 (1H, 2d, J = 9.0 Hz), 7.52-7.49 and 7.51-7.48 (1H, 2d, J = 9 Hz,), 7.00 and 6.99 (1H, 2s), 6.72 (2H, s), 6.51 (2H, s), 4.12 (3H, s), 3.96 and 3.93 (3H, 2s), 3.74 (6H, s), 3.35 (6H, s); ^{13}C NMR δ 168.8, 168.6, 152.8, 149.28, 149.25, 149.18, 149.14, 148.15, 135.53, 135.41, 134.7, 132.1, 132.0, 131.4, 131.3, 131.2, 131.16, 131.0, 130.43, 130.36, 129.6, 129.2, 129.0, 128.2, 127.6, 126.9, 126.8, 126.1, 125.8, 125.7, 125.3, 125.2, 125.1, 124.9, 122.6, 122.5, 115.0, 114.9, 113.9, 109.7, 104.3, 104.23, 104.16, 103.4, 56.4, 56.1, 55.7, 55.6, 55.43, 55.37. MS –TOF calcd for $C_{43}H_{34}O_8$ 678.23, found m/z 677.3 (M-1). HRMS ESI MH^+ calcd for $C_{43}H_{35}O_8$ 679.2332, found 679.2289 . FTIR (neat): ν 3527 (br) 2920, 2851, 1738 and 1717 (atropisomer C=O's), 1461, 1260 cm^{-1}; Tg=130.13°C, Tm=228.78°C, Td=348.37°C. Tg=120-125°C. The individual atropisomers were separated by preparative plate chromatography to afford the two separate atropisomers of **4c**: ^{1}H NMR for second eluted isomer δ 8.41 (1H, d, J=7.9 Hz), 8.28 (1H, dd, J=7.9, 4.0 Hz, 3.9 Hz), 8.23 (2H, d, J = 4.4 Hz), 8.04 (1H, t, J = 8.0 Hz), 8.12 (2H, m), 7.90 (1H, s), 7.83 (1H, d, J = 9.2 Hz) d), 7.49 (1H, d, J = 9.2 Hz), 6.99 (1H, s), 6.75 (2H, s), 6.50 (2H, s), 4.12 (3H, s), 3.96 (3H, s), 3.75 (6H, s), 3.35 (6H, s).

(4,5-dimethoxy-2-(2,3,6,7-tetramethoxy-10-phenylanthracen-9-yl)phenyl)methanol (5a). Phenyl anthracene derivative **4a** (122 mg, 0.22 mmol) was dissolved in THF (0.4 mL). A

solution of lithium aluminum hydride (0.45 mL, 0.45 mmol, 1.0 M in THF) was added gradually via syringe and the reaction was then heated to reflux under nitrogen for 19 h. It was then allowed to cool to room temperature and diluted with 15% aqueous sodium hydroxide (1.0 mL), stirred for 10 min and then diluted with THF (1.0 mL) followed by water (1.0 mL). The reaction was dried over $MgSO_4$, filtered, and washed successively with THF, dichloromethane and ethyl acetate. Concentration under reduced pressure afforded a residue which was purified by silica gel column chromatography eluting with toluene/dichloromethane and dichloromethane/ether (100% to 10 % with 10 % increments for each interval) to obtain **5a** as a light orange solid product (92.6 mg, 88%): ^{1}HNMR (500 MHz, $CDCl_3$) δ 7.63–7.45 (5H, m), 7.29 (1H, s), 6.87 (1H, s), 6.83 (2H, s), 6.70 (2H, s), 4.24 (2H, s), 4.07 (3H, s), 3.86 (3H, s), 3.74 (6H, s), 3.73(6H, s); ^{13}C NMR δ 149.0, 148.7, 148.3, 148.2, 139.23, 139.14, 133.1, 132.3, 130.6, 130.1, 129.6, 129.4, 128.3, 127.2, 125.8, 125.5, 113.43, 113.39, 110.9, 103.9, 103.8, 102.94, 102.88, 62.8, 55.8, 55.7, 55.5, 55.4, 55.3, 55.2, 55.1. HRMS-TOF m/z calcd for $[C_{33}H_{32}O_7]+Na^+$ 563.2046, found 563.2048 ($M+Na^+$); FTIR (neat): ν 3498 (br) 2916, 2848, 1489, 1235 cm^{-1}; Tg =165.6ºC. Tm=197-203ºC.

(4,5-Dimethoxy-2-(2,3,6,7-tetramethoxy-10-(naphthalen-2-yl)anthracen-9-yl)phenyl)methanol (5b). Naphthyl anthracene derivative **4b** (88 mg, 0.145 mmol) was dissolved in THF (0.29 mL). A solution of lithium aluminum hydride (0.29 mL, 0.29 mmol, 1.0 M in THF) was added gradually by a syringe and the reaction was heated under reflux under nitrogen for 24 h. The reaction was then allowed to cool to room temperature and diluted with aqueous 15% sodium hydroxide (1.0 mL), stirred for 10 min and then diluted with THF (1.0 mL) followed by 1.0 mL water, dried with MgSO4, filtered and washed with THF, dichloromethane and ethyl acetate, then concentrated under reduced pressure and purified by silica gel column chromatography eluting with toluene/dichloromethane and dichloromethane/ether (100% to 10 % with 10 % increments for each interval) to obtain **5b** as a light orange solid product (85.9 mg, 100%): ^{1}H NMR (500 MHz, $CDCl_3$) δ 8.07 (1H, dd, J = 8.4, 3.9 Hz), 8.04-7.92 (3H, m), 7.68-7.56 (3H, m), 7.31 (1H, s), 6.891 and 6.886 (1H, two s, atropisomers), 6.86 (2H, s), 6.73 (2H, s), 4.26 (2H, s), 4.08 (3H, s), 3.874 and 3.872 (3H, two s, atropisomers), 3.74 (6H, s), 3.64 (6H, s), 2.30 (1H,s); ^{13}C NMR δ 149.6, 149.4, 148.9, 148.8, 137.4, 137.37, 134.0, 133.4, 133.0, 132.93, 130.8, 130.3, 130.2, 129.6, 129.3, 128.6, 128.5, 128.4, 128.2, 126.6, 126.5, 126.3, 125.6,

114.0, 114,0, 111.6, 104.5, 104.4, 103.6, 103.57, 63.5, 56.4, 56.2, 56.0, 55.96, 55.88, 55.83; HRMS-ESI calcd for $C_{37}H_{34}O_7$ 590.2299, m/z found 590.2293 (M+); M-OH calcd for $C_{37}H_{33}O_6$ 573.2272, m/z found 573.2279 $(M\text{-}OH)^+$; M+Na+ calcd for $C_{37}H_{34}O_7Na$ 613.2197, m/z found 613.2188 $(M+Na^+)$. Tm=202-205^{o}C.

(4,5-dimethoxy-2-(2,3,6,7-tetramethoxy-10-(pyren-1-yl)anthracen-9-yl)phenyl)methanol (5c). Pyrenyl adduct **4c** (56.4 mg, 0.085 mmol) was dissolved in THF (0.4 mL). A solution of lithium aluminum hydride (0.37 mL, 0.37 mmol, 1.0M in THF) was added gradually by a syringe and the reaction was heated under reflux for 24 h. The reaction was then allowed to cool to room temperature and was diluted with 15% aqueous sodium hydroxide (1.0 mL), stirred for 10 min and then diluted with THF (1.0 mL) followed by water (1.0 mL). The reaction was dried over $MgSO_4$, filtered, and washed with THF, dichloromethane, and ethyl acetate, concentrated under reduced pressure and the resulting residue was purified by silica gel column chromatography eluting with toluene/dichloromethane and ether to obtain a light orange solid product (54.2 mg, 96%): ^{1}H NMR (mixture of atropisomers) δ 8.44–8.42 and 8.43-8.40 (1H, 2d, J = 7.8 Hz), 8.30-8.00 (6H, m), 7.90 and 7.86 (1H, 2d, J = 9.3 Hz), 7.53- 7.50 and 7.51-7.48 (1H, 2d, J = 9.3 Hz), 7.36-7.34 (1H, d, J = 5.7 Hz), 7.01 and 6.97 (1H, 2s), 6.80 (2H,s), 6.52 (2H, s), 4.40 and 4.30 (2H, 2s), 4.12 (3H, s), 3.94 and 3.91 (3H, 2s), 3.77 (6H, s), 3.37 (6H, s). ^{13}CNMR δ 149.7, 149.5, 148.9, 134.8, 132.9, 131.7, 131.6, 131.4, 131.3, 131.2, 130.6, 130.3, 129.5, 127.9, 127.2, 126.5, 126.0, 125.5, 125.3, 125.2, 114.0, 104.5, 103.6, 88.6, 88.1, 87.7, 63.6, 56.4, 56.2, 56.0, 55.7. HRMS-ESI m/z calcd for $C_{43}H_{36}O_7$ 664.2456, found 664.2456; M-OH calcd for $C_{43}H_{35}O_6$ (M-OH) 647.2428, found 647.2446; calcd for $C_{43}H_{36}O_7Na$ $(M+Na^+)$ 687.2353, found 687.2356. Tg=115-120^{o}C.

Dedication

Dedicated to the memory of the late Professor Howard E. Zimmerman.

Acknowledgements

NSF Grant DBI-0216630 is gratefully acknowledged for the Varian UNITY-300 NMR obtained through the NSF Biological Major Instrumentation Program. The X-ray diffractometer was

funded by NSF Grant 0087210, Ohio Board of Regents Grant CAP-491, and by Youngstown State University.

Supporting information. Includes copies of spectral data (^{1}H NMR, ^{13}C NMR, IR and HRMS), X-ray structure orteps of ethyl ester **3b**, and complete X-ray crystallography tables for both bromoanthracenes **3a** and **3b**. This material is available free of charge via the Internet at http://pubs.acs.org. CCDC 899435 & 899436 contain the supplementary crystallographic data for this paper. These data can be obtained free of charge from The Cambridge Crystallographic Data Centre via www.ccdc.cam.ac.uk/data_request/cif.

References

(1) Kim, Y.; Bae, K. H.; Jeong, Y. Y.; Choi, D. K.; Ha, C. *Chem. Mater.* **2004**, *16*, 5051-5057.
(2) Leo, K. *Nat. Photonics* **2011**, *5*, 716-718.
(3) Patra, A.; Pan, M.; Friend, C. S.; Lin, T.; Cartwright, A. N.; Prasad, P. N.; Burzynski, R. *Chem. Mater.* **2002**, *14*, 4044-4048.
(4) Reineke, S.; Lindner, F.; Schwartz, G.; Seidler, N.; Walzer, K.; Luessem, B.; Leo, K. *Nature (London, U. K.)* **2009**, *459*, 234-238.
(5) Cho, I.; Kim, S. H.; Kim, J. H.; Park, S.; Park, S. Y. *J. Mater. Chem.* **2012**, *22*, 123-129.
(6) Danel, K.; Huang, T.; Lin, J. T.; Tao, Y.; Chuen, C. *Chem. Mater.* **2002**, *14*, 3860-3865.
(7) Shi, J.; Tang, C. W. *Appl. Phys. Lett.* **2002**, *80*, 3201-3203.
(8) Balaganesan, B.; Shen, W.; Chen, C. H. *Tetrahedron Lett.* **2003**, *44*, 5747-5750.
(9) Tao, S.; Hong, Z.; Peng, Z.; Ju, W.; Zhang, X.; Wang, P.; Wu, S.; Lee, S. *Chem. Phys. Lett.* **2004**, *397*, 1-4.
(10) Tao, S.; Xu, S.; Zhang, X. *Chem. Phys. Lett.* **2006**, *429*, 622-627.
(11) Zhu, M.; Ye, T.; Li, C.; Cao, X.; Zhong, C.; Ma, D.; Qin, J.; Yang, C. *J. Phys. Chem. C* **2011**, *115*, 17965-17972.
(12) Wu, C.; Chien, C.; Hsu, F.; Shih, P.; Shu, C. *J. Mater. Chem.* **2009**, *19*, 1464-1470.
(13) Zheng, C.; Zhao, W.; Wang, Z.; Huang, D.; Ye, J.; Ou, X.; Zhang, X.; Lee, C.; Lee, S. *J. Mater. Chem.* **2010**, *20*, 1560-1566.
(14) Kim, H. S.; Tsutsui, T. *J. Ind. Eng. Chem. (Seoul)* **1998**, *4*, 324-328.
(15) Panagopoulos, A. M.; Zeller, M.; Becker, D. P. *J. Org. Chem.* **2010**, *75*, 7887-7892.
(16) French, D. C.; Lutz, M. R., Jr.; Lu, C.; Zeller, M.; Becker, D. P. *J. Phys. Chem. A* **2009**, *113*, 8258-8267.
(17) Zeller, M.; Lutz, M. R., Jr.; Becker, D. P. *Acta Crystallogr., Sect. B: Struct. Sci.* **2009**, *B65*, 223-229, S223/1-S223/10.
(18) Collet, A. *Tetrahedron* **1987**, *43*, 5725-5759.
(19) Osner, Z. R.; Nyamjav, D.; Holz, R. C.; Becker, D. P. *Nanotechnology* **2011**, *22*, 275611/1-275611/6, S275611/1-S275611/3.
(20) Cookson, R. C.; Halton, B.; Stevens, I. D. R. *J. Chem. Soc. B: Phys. Org.* **1968**, 767-774.

(21) Lutz, M. R., Jr.; Zeller, M.; Becker, D. P. *Acta Crystallographica, Section E: Structure Reports Online* **2007**, *E63*, o3857-o3858.
(22) Lutz, M. R., Jr.; Zeller, M.; Becker, D. P. *Tetrahedron Lett.* **2008**, *49*, 5003-5005.
(23) Nishihara, Y.; Onodera, H.; Osakada, K. *Chem Commun (Camb)* **2004**, 192-193.
(24) Qiu, W.; Chen, S.; Sun, X.; Liu, Y.; Zhu, D. *Org. Lett.* **2006**, *8*, 867-870.
(25) Weibel, J.; Blanc, A.; Pale, P. *Chem. Rev. (Washington, DC, U. S.)* **2008**, *108*, 3149-3173.
(26) Cammidge, A. N.; Crepy, K. V. L. *J. Org. Chem.* **2003**, *68*, 6832-6835.
(27) Nikitin, K.; Muller-Bunz, H.; Ortin, Y.; Muldoon, J.; McGlinchey, M. J. *Org. Lett.* **2011**, *13*, 256-259.
(28) Suzuki, T.; Nagano, M.; Watanabe, S.; Ichimura, T. *J. Photochem. Photobiol. A* **2000**, *136*, 7-13.
(29) Hamilton, T. D. S. *Photochem. Photobiol.* **1964**, *3*, 153-156.
(30) Weigel, W.; Rettig, W.; Dekhtyar, M.; Modrakowski, C.; Beinhoff, M.; Schlueter, A. D. *J. Phys. Chem. A* **2003**, *107*, 5941-5947.
(31) Klock, A. M.; Rettig, W.; Hofkens, J.; van Damme, M.; De Schryver, F. C. *J. Photochem. Photobiol. , A* **1995**, *85*, 11-21.
(32) Baumgarten, M.; Gherghel, L.; Friedrich, J.; Jurczok, M.; Rettig, W. *J. Phys. Chem. A* **2000**, *104*, 1130-1140.
(33) Meech, S. R.; Phillips, D. *J. Photochem.* **1983**, *23*, 193-217.
(34) Crosby, G. A.; Demas, J. N. *J. Phys. Chem.* **1971**, *75*, 991-1024.
(35) Williams, A. T. R.; Winfield, S. A.; Miller, J. N. *Analyst (London)* **1983**, *108*, 1067-1071.
(36) Parker, C. A.; Rees, W. T. *Analyst* **1960**, *85*, 587-600.
(37) Dawson, W. R.; Windsor, M. W. *J. Phys. Chem.* **1968**, *72*, 3251-3260.
(38) Moorthy, J. N.; Venkatakrishnan, P.; Natarajan, P.; Huang, D.; Chow, T. J. *J. Am. Chem. Soc.* **2008**, *130*, 17320-17333.
(39) Ricci, R. W.; Nesta, J. M. *J. Phys. Chem.* **1976**, *80*, 974-980.
(40) Park, H.; Lee, J.; Kang, I.; Chu, H. Y.; Lee, J.; Kwon, S.; Kim, Y. *J. Mater. Chem.* **2012**, *22*, 2695-2700.
(41) Yokota, K.; Hagimori, M.; Mizuyama, N.; Nishimura, Y.; Fujito, H.; Shigemitsu, Y.; Tominaga, Y. *Beilstein J. Org. Chem.* **2012**, *8*, 266-274, No. 28.
(42) Langhals, H.; Potrawa, T.; Noeth, H.; Linti, G. *Angew. Chem.* **1989**, *101*, 497-499.
(43) Nishiguchi, N.; Kinuta, T.; Sato, T.; Nakano, Y.; Harada, T.; Tajima, N.; Fujiki, M.; Kuroda, R.; Matsubara, Y.; Imai, Y. *Cryst. Growth Des.* **2012**, *12*, 1859-1864.
(44) Anthony, S. P.; Varughese, S.; Draper, S. M. *J. Phys. Org. Chem.* **2010**, *23*, 1074-1079.
(45) Yu, Y.; Shi, Q.; Li, Y.; Liu, T.; Zhang, L.; Shuai, Z.; Li, Y. *Chem Asian J* **2012**.
(46) Hamilton, T. D. S. *Photochem. Photobiol.* **1964**, *3*, 153-156.
(47) Lutz Jr., M. R.; French, D. C.; Rehage, P.; Becker, D. P. *Tetrahedron Letters* **2007**, *48*, 6368-6371.
(48) Zhang, M.; Li, K.; Pan, Z.; Jin, X.; Tang, Y. *Beijing Daxue Xuebao, Ziran Kexueban* **1989**, *25*, 138-145.

TOC Graphic

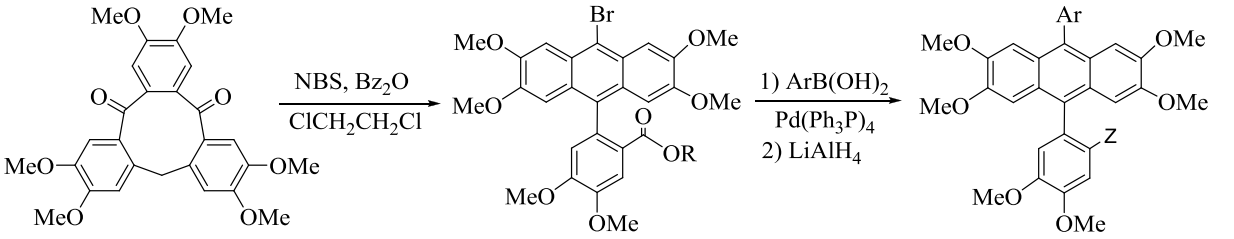

1a
CTV diketone

3a R = H
3b R = ethyl

Ar = Ph, 2-naphthyl, 1-pyrenyl
Z = CO_2H (**4a-c**), CH_2OH (**5a-c**)

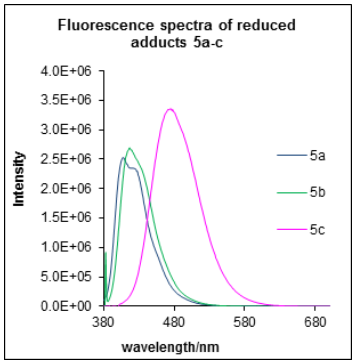

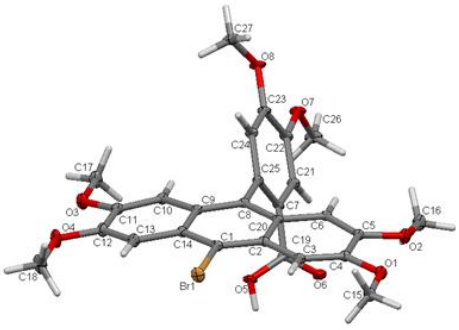

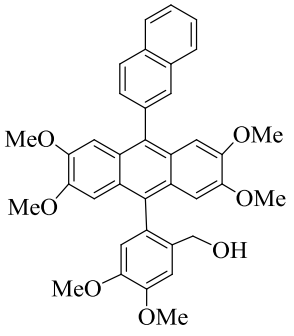

5b
quantum yield = 39%